Mice conditionally expressing RET(C618F) mutation display C cell hyperplasia and hyperganglionosis of the enteric nervous system

Mitsumasa Okamoto[1, 2], Yuta Yoshioka[1, 3], Kosaku Maeda[4], Yuko Bito[5], Takumi Fukumoto[3], Toshihiro Uesaka[1] and Hideki Enomoto[1]

[1] Division for Neural Differentiation and Regeneration, Department of Physiology and Cell Biology, Kobe University Graduate School of Medicine, Kobe, Hyogo, Japan

[2] Department of Pediatric Surgery, Takatsuki General Hospital, Takatsuki, Osaka, Japan

[3] Division of Hepato-Biliary-Pancreatic surgery, Department of Physiology and Cell Biology, Kobe University Graduate School of Medicine, Kobe, Hyogo, Japan

[4] Department of Surgery, Hyogo Prefectural Kobe Children's Hospital, Kobe, Hyogo, Japan

[5] Division of Pediatric Surgery, Department of Surgery, Kobe University Graduate School of Medicine, Kobe, Hyogo, Japan

Correspondence
Hideki Enomoto, Division for Neural Differentiation and Regeneration, Department of Physiology and Cell Biology, Kobe University Graduate School of Medicine
7-5-1 Kusunoki-cho, Chuo-ku, Kobe, Hyogo 650-0017, Japan.
Email: enomotoh@med.kobe-u.ac.jp

Funding information
KAKENHI (Grants-in-Aid for Scientific Research), Grant Numbers: JP17H03550 (HE), 17K19527 (HE), and 16K08466 (TU).
Yakult Bio-Science Foundation (HE).
Takeda Science Foundation (HE).

Summary

Medullary thyroid carcinoma (MTC) develops from hyperplasia of thyroid C cells and represents one of the major causes of thyroid cancer mortality. Mutations in the cysteine-rich domain (CRD) of the *RET* gene are the most prevalent genetic cause of MTC. The current consensus holds that such cysteine mutations cause ligand-independent dimerization and constitutive activation of RET. However, given the number of the CRD mutations left uncharacterized, our understanding of the pathogenetic mechanisms by which CRD mutations lead to MTC remains incomplete. We report here that RET(C618F), a mutation identified in MTC patients, displays moderately high basal activity and requires the ligand for its full activation. To assess the biological significance of RET(C618F) in organogenesis, we generated a knock-in mouse line conditionally expressing RET(C618F) cDNA by the *Ret* promoter. The RET(C618F) allele can be made to be Ret-null and express mCherry by Cre-loxP recombination, which allows the assessment of the biological influence of RET(C618F) in vivo. Mice expressing RET(C618F) display mild C cell hyperplasia and increased numbers of enteric neurons, indicating that RET(C618F) confers gain-of-function phenotypes. This mouse line serves as a novel biological platform for investigating pathogenetic mechanisms involved in MTC and enteric hyperganglionosis.

KEYWORDS

Medullary thyroid carcinoma, C cell hyperplasia, knock-in, disease model, reporter line, Ret mutant

Medullary thyroid carcinoma (MTC) represents a small fraction (~3%) of all thyroid cancers (Accardo et al., 2017). MTC is associated with poor prognosis and accounts for a substantial fraction of thyroid cancer mortality. Understanding the pathogenesis of MTC should provide important information for the development of novel strategies for the treatment and prevention of this disease.

About 25% of MTC cases are hereditary and occurs in multiple endocrine neoplasia syndrome (MEN) 2, which is further subcategorized into MEN2A, MEN2B and familial MTC (FMTC) based on its association with pheochromocytoma, hyperparathyroidism, and/or other developmental anomalies (e.g. infertility, marfanoid habitus, mucosal neuromas, intestinal ganglioneuroma etc.). MEN2A and MEN2B are caused by germ-line mutations of the rearranged during transformation (*RET*) gene (Mulligan et al., 1993) (Carlson et al., 1994). In MEN2A and FMTC, point mutations affecting six cysteine residues (C609, 611, 618, 620, 630, 634) in the cysteine-rich domain (CRD) of the extracellular region of RET induce oncogenic transformation. Elegant biochemical analyses of C634 mutations revealed ligand-independent dimerization and auto-activation of RET, providing mechanistic insights into how CRD mutations leads to constitutive activation of RET (Asai, Iwashita, Matsuyama, & Takahashi, 1995) (Santoro et al., 1995). The prevailing model holds that cysteine residues in the CRD are crucial for the formation of the tertiary structure via intermolecular di-sulfide bonding, and that substitution of a single C634 residue by another amino acid residue leaves its partner cysteine unpaired, which results in the formation of intermolecular disulfide bonding between RET without ligands. Although this model is widely accepted, detailed characterization has been performed mostly on the C634 mutation. There are a number of mutations affecting other cysteine residues, and the picture of biological effects by CRD mutations remains incomplete.

MTC develops from thyroid C cells, which produce calcitonin. Pathological analyses have revealed that C cell hyperplasia (CCH) precedes MTC (Wolfe et al., 1973), suggesting a step-wise oncogenesis of MTC via CCH. Transgenic mice overexpressing RET(C634R) by the calcitonin promoter display MTC and CCH, indicating that RET(C634R) is sufficient to cause oncogenic changes in vivo (Michiels et al., 1997) (Reynolds et al., 2001). However, in these models, expression of RET(C634R) is driven by artificial promoters, not by the endogenous *Ret* promoter, leaving the possibility that spatiotemporal expression of the RET(C634R) may not be recapitulated. Given that

recent strategies for the treatment and/or prevention of MTCs involve the use of RET inhibitors, defining the timing of malignant transformation in C cells by mutant RET is crucial for optimizing the treatment strategy. To this end, animal models more faithfully recapitulating human MTCs or CCH are required.

In the present study, we investigated the biological properties of RET(C618F), one of the RET CHD mutants that has been identified in MTC patients (Wells et al., 1994). Biochemical analysis revealed that RET(C618F) showed higher basal phosphorylation than normal and required ligand stimulation for its full activation. To assess its biological significance in vivo, we generated a knock-in mouse line that conditionally expresses RET(C618F) under the *Ret* promoter. Mice expressing RET(C618F) developed CCH and hyperganglionosis of the enteric nervous system, demonstrating the gain-of-function effects induced by RET(C618F). In this mouse line, expression of RET(C618F) can be attenuated by Cre-loxP recombination, which makes it possible to determine the time window of RET(C618F) expression required for gain-of-function effects. Our conditional RET(C618F) knock-in mouse line provides a unique biological platform to understand the pathogenetic mechanisms of MTC.

1. RESULTS AND DISCUSSION

To understand the biological effects of CRD mutations that were not well characterized previously, we chose the C618F, C618R and C620R mutants (Figure 1A). These mutants have been identified in MEN2A patients and are known to exert low to intermediate transforming activity in vitro (Carlomagno et al., 1997) (Ito et al., 1997). We infected a lentivirus vector designed to express wild-type (wt) RET51 (a long isoform of RET) or one of the target mutations to CHP126 cells, a neuroblastoma cell line expressing GFRα1 (Tsui-Pierchala, Ahrens, Crowder, Milbrandt, & Johnson, 2002) receptor. Although wt RET51 showed elevated RET phosphorylation after GDNF treatment (Figure 1B, lanes 1 and 2), RET51(C618R) and RET51(C620R) already displayed high levels of basal phosphorylation of RET in the absence of ligand, and no additional elevation of phosphorylation was observed following GDNF treatment (Figure 1B, lanes 5-8). In contrast, RET51(C618F) showed moderate basal RET phosphorylation, and phosphorylation levels significantly increased after GDNF treatment (Fig. 1B, lanes 3 and 4). Biotinylation of cell surface proteins revealed that both RET51(C618R) and RET51(C620R) failed to localize at the plasma membrane (Fig. 1C), whereas wt

RET51 and RET51(C618F) are expressed at the cell surface, as normal (Fig. 1C). These data reveal distinct biochemical properties among C618 and C620 mutants and demonstrate that RET51(C618F) is a GDNF-responsive RET-activating mutant.

To understand the physiological influences of RET51(C618F) in vivo, we inserted a gene cassette composed of floxed-human *RET51(C618F)* cDNA followed by mCherry cDNA and frt-franked neomycin-resistance gene into the mouse *Ret* locus by gene targeting (Figure 2). We engineered the *Ret* allele such that *RET51(C618F)* is expressed under the endogenous *Ret* promoter and can be removed by Cre-mediated recombination. This conditional deletion strategy allows us to assess the spatiotemporal requirement for RET51(C618F) in any observed phenotype in mouse. As a control, we adopted the same strategy and generated mice expressing wt RET51, instead of RET51(C618F). Mice heterozygous for the RET51 or RET51(C618F) allele (hereafter referred to as $Ret^{51/+}$ or $Ret^{51(C618F)/+}$) were born and grew with no apparent abnormal phenotypes.

To assess whether human RET cDNA is properly expressed, we examined the enteric nervous system, as ENS precursors physiologically express RET. The gut was subjected to immunostaining using human-specific anti-RET antibodies (anti-hRET). To reveal the presence of ENS precursors, antibodies against Phox2B, a transcription factor highly expressed in all ENS precursors, were used. As shown in Figure 3A and B, anti-hRET stained the plasma membrane and cytoplasm (green) of all enteric neurons in which the nuclei were detected by anti-Phox2B (red) in the gut of $Ret^{51(C618F)/51(C618F)}$ mice. In contrast, no hRET signal was detected in the control ($Ret^{+/+}$ mice). Similar human-specific RET staining was observed in $Ret^{51/51}$ gut (data not shown). These data indicate expression of human RET proteins by these conditional alleles.

We next evaluated conditional attenuation of hRET expression. Both *RET51* and *RET51(C618F)* alleles are designed to induce expression of mCherry after the removal of the floxed *RET* cDNA by Cre-mediated recombination. We therefore crossed $Ret^{51/+}$ or $Ret^{51(C618F)/+}$ mice to *β-actin Cre* (*Actb::Cre*) mice, a global deleter mouse line (Figure 3B). In double compound animals ($Ret^{51/+}$; *Actb::Cre* or $Ret^{51(C618F)/+}$; *Actb::Cre*), we observed strong mCherry expression in enteric neurons and the ureteric buds of developing kidneys (Figure 3C), a pattern that faithfully recapitulates the endogenous expression of the *Ret* gene. This cross established a new Ret knockin line that express

mCherry under the *Ret* promoter. Finally, consistent with the fact that RET is essential for the development of the enteric nervous system and kidneys (Schuchardt, D'Agati, Larsson-Blomberg, Costantini, & Pachnis, 1994), $Ret^{mCherry/mCherry}$ mice displayed intestinal aganglionosis and kidney agenesis (data not shown). Together, these data validate the physiologic expression of RET, conditional attenuation of hRET expression, and recombination-induced induction of mCherry expression in both *RET51* and *RET51(C618F)* alleles.

To understand the biological influence of RET51(C618F) in vivo, we first sought to examine the phenotype of $Ret^{51(C618F)/51(C618F)}$ mice, because full activation of RET by C618F mutation was expected in these animals. Although $Ret^{51(C618F)/51(C618F)}$ mice were born nearly at the expected Mendelian ratio, all died within 24 hours after birth. Kidney agenesis and intestinal aganglionosis, a hallmark of RET deficiency, did not occur in any of $Ret^{51(C618F)/51(C618F)}$ mice (Figure 4), indicating that RET51(C618F) does not exert any loss-of-function effects in the development of the kidney and ENS. Wholemount staining of the small intestine and colon with anti-Phox2B antibodies revealed that the density of enteric neurons was noticeably higher in $Ret^{51(C618F)/51(C618F)}$ mice than $Ret^{51/51}$ mice (Figure 4A; data not shown). Although the precise cause of neonatal death in $Ret^{51(C618F)/51(C618F)}$ mice remains unknown, the data clearly demonstrate gain-of-function effects of RET51(C618F) in vivo.

We next conducted histological analyses on the ENS and the thyroid tissues of $Ret^{51/+}$ and $Ret^{51(C618F)/+}$ mice. We found that the numbers of enteric neurons were significantly increased in $Ret^{51(C618F)/+}$ mice as compared to $Ret^{51/+}$ mice (Figure 5A and B, myenteric plexus of the proximal small intestine P0). Because GDNF-mediated RET activation is required for proliferation of the ENS precursors, this result suggests that RET51(C618F) enhances proliferation of ENS precursors in vivo. Further studies are needed to verify this assumption. To address whether similar effects are observed in thyroid C cells, we performed in situ hybridization analysis on consecutive sections of thyroid tissue from 1-year-old mice using riboprobes detecting gene expression of calcitonin, a hormone secreted from thyroid C cells. In $Ret^{51/+}$ mice, C cells were found relatively evenly scattered in the interstitial space of the thyroid follicles (Figure 5C, left). In contrast, C cells were more unevenly distributed and occasionally formed dense patches $Ret^{51(C618F)/+}$ mice (Figure 5C, right). Measuring the entire areas with calcitonin signals revealed that this area tends to be larger in $Ret^{51(C618F)/+}$ mice than in $Ret^{51/+}$ mice.

However, this overall comparison did not reach statistical significance (Figure 5D), suggesting that C cell abnormality occurs only focally, not ubiquitously. Therefore, we examined the numbers of follicles that were completely surrounded by multiple layers of C cells, a feature observed in C cell hyperplasia. This analysis detected a statistically significant increase in the number of affected follicles in *Ret*$^{51(C618F)/+}$ mice (Figure 5E, p=0.028). In summary, mice harboring the RET51(C618F) allele display increased numbers of enteric neurons and mild focal C cell hyperplasia, which is consistent with the biochemical properties of RET51(C618F).

In this study, we generated a new mouse model for MEN2A harboring RET51(C618F) mutation. Our biochemical analysis revealed that RET51(C618F) is expressed on the cell surface, and its phosphorylation is enhanced by GDNF treatment. Mice expressing RET51(C618F) via the endogenous *Ret* promoter displayed hyper-ganglionosis of the gut and C cell hyperplasia (CCH), demonstrating that RET51(C618F) exerts gain-of-function effects in vivo. Although focal C cell hyperplasia is present throughout the thyroid gland of *Ret*$^{51(C618F)/+}$ mice, we have obtained no evidence of MTC development in these animals (up to two years). Moreover, no overt tumorigenesis was detected in the adrenal medulla, a feature observed in MEN2A patients. This may be consistent with the results of a previous study, which showed that RET(C618X) displays significantly lower transforming activity than RET(C634X), a mutation found in the most aggressive form of MEN2A. Nonetheless, our RET51(C618F) mice provide a unique platform for studying the pathogenesis of MTC. First, development of CCH in these mice suggest that CCH can occur in a ligand-dependent fashion in some MEN2A patients. Since RET can be activated by GDNF Family ligands (GFLs) that include four members, identification of the exact ligand responsible for CCH development may open a new corridor for drug development. Moreover, conditional deletion of RET51(C618F) in these animals will reveal the temporal window in which RET activation is required for the development of CCH. Such analysis will provide vital information as to when RET activation must be switched off in C cells to prevent the development of CCH. Such knowledge is especially important noting that the use of RET inhibitors has been attracting a great deal of attention as a novel therapeutic strategy for the treatment of MTC.

RET51(C618F) mice can also be used to address many biological questions regarding the development of the enteric nervous system (ENS). We assume that the increased number of enteric neurons observed in the ENS of *Ret*$^{51(C618F)/+}$ mice is caused

by combinatorial effects of the cell surface expression, high basal activity, and GDNF-responsiveness of RET51(C618F). Although several mouse lines expressing activating RET mutations, including C620R, C634R, M918T, have been reported (Michiels et al., 1997) (Acton, Velthuyzen, Lips, & Hoppener, 2000) (Reynolds et al., 2001) (Carniti et al., 2006) (Yin et al., 2007), *Ret*$^{51(C618F)/+}$ mice are the first mouse line, to our knowledge, that displays increased numbers of enteric neurons by a *Ret* mutation. Because development of the ENS is highly sensitive to levels of RET/GDNF signaling, this mouse line can be utilized to study the biological influences of slightly elevated RET signaling on ENS precursors, which is important for understanding the pleiotropic and long-term actions of GDNF and RET in ENS development.

2. METHODS

2.1 *Cloning*

Each cysteine mutation of human RET 51 (C618F, C618R, and C620R) was introduced by standard PCR-based site-directed mutagenesis method. Primers containing the mutations were synthesized and used for amplification of human *Ret 51* cDNA inserted into the pcDNA3.1 (Thermo Fisher Scientific). PCR products were transformed into competent *Escherichia coli* cells, and then the mutagenized plasmid was taken up. The inserted *Ret 51* cDNA was sequenced to confirm that proper mutations were introduced.

2.2 *Lentiviral vector design and production*

A self-inactivating third-generation lentiviral vector, FUW (Lois, Hong, Pease, Brown, & Baltimore, 2002) was used in this study. To make FUW-IRES-Puro, *IRES-puromycin N-acetyl-transferase* cDNA from pCAP-EGFP (provided by M. Takeichi, RIKEN, Kobe) was cloned downstream of the human polyubiquitin promoter-C in the plasmid FUW. Wild-type or mutant forms of *Ret 51* cDNA were cloned between the polyubiquitin promoter-C and IRES sequence.

Ret-expressing lentiviruses were generated by calcium phosphate precipitation transfection of 34 μg of the lentiviral transfer vector plasmid (FUW), 24 μg of the envelope plasmid (pCMV-VSV-G), and packaging plasmids (20 μg of pMDLg/pRRE and 20 μg of pRSV-Rev) into 293T cells. After 48 hr post-transfection, the viral supernatants were harvested and filtered through a 0.45 μm filter (Milex-HP, Merck). To concentrate the viral particles, the supernatants were ultracentrifugated (CR21N, Hitachi, Japan) at 44200 × g for 2 hr. The viral pellets were resuspended in 100 μl of cold PBS.

2.3 *Cell line construction*

CHP126 human neuroblastoma cells, which do not express endogenous *Ret* (Crowder et al., 2004), were used to produce cell lines stably expressing wild-type or mutant RET51 isoforms. CHP126 cells were infected with lentiviruses containing wild-type or mutant RET 51 isoforms, incubated for 48 h in the growth medium (10% fetal bovine serum (FBS, Thermo Fisher scientific), penicillin and streptomycin (Meiji) in DMEM/Ham's F-12 with L-Glutamine (Wako), and selected by puromycin to obtain stable lines.

2.4 *Gene targeting in ES cells*

The wild-type or mutant alleles of human RET51 C618F (*Ret*^{51} or *Ret*$^{51(C618F)}$) were generated by knocking a gene cassette composed of floxed human *Ret*^{51} (or *Ret*$^{51(C618F)}$) cDNA-*SV40 intron polyA* followed by mCherry reporter and a neomycin resistance marker (*Neo*) that was flanked by *FRT* sites (*loxP-Ret*^{51} [or *Ret*$^{51(C618F)}$]-*loxP-mCherry-FRT Neo FRT* cassette) into the first coding exon of the *Ret* gene. This strategy was identical to that described previously (Enomoto et al., 2001). 129sv-derived embryonic stem cells (EB3) were cultured on GMEM (Sigma) supplemented with 10% FBS, 1 non-essential amino acids (NEAA, Thermo Fisher Scientific), 1 mM sodium pyruvate, 1000 units/ml leukemia inhibitory factor (LIF), and 0.1 mM 2-mercaptoethanol. 1×10^7 cells were electroporated with 15 μg of linearized targeting construct. After electroporation, the cells were exposed to G418 (300 μg/ml, Sigma). The colonies were picked, and further expanded by growing on 96-well plates. The ES clones were screened by a locus-specific PCR. The ES cell clones with properly inserted targeting vector were further screened by Southern blotting.

2.5 *Generation of Ret*^{51} *or Ret*$^{51(C618F)}$ *knock-in mice*

The targeted ES cell clones were injected into C57BL/N6 mouse blastocysts, and chimeric mice were generated. Chimeric mice were bred to transgenic mice expressing Flp recombinase to delete *Neo* and mice harboring *Ret*^{51} or *Ret*$^{51(C618F)}$ were produced. These mice were backcrossed into the C57BL/6N for 10 generations. *Ret*$^{51/+}$ mice were crossed with *Actb::Cre* strain (Jackson Lab.) to generate *Ret-mCherry* knock-in mice. Mice were bred and maintained at the Institute of Experimental Animal Research of Kobe University Graduate School of Medicine under specific pathogen-free conditions and all animal experiments were performed according to Kobe University Animal Experimentation Regulations. *Ret*^{51}, *Ret*$^{51(C618F)}$ and *Ret-mCherry* knock-in mice will be available to the scientific community upon request. Contact LARGE (Laboratory for Animal Resources and Genetic Engineering.) in RIKEN Center for Biosystems Dynamics Research (http://www2.clst.riken.jp/arg/mutant%20mice%20list.html) for the mouse transfer. The official names (ID) of *Ret*^{51} and *Ret*$^{51(C618F)}$ mice are Ret-flox RET51 mCherry (CDB1384K) and Ret-flox RET51(C618F) mCherry (CDB1385K), respectively.

2.6 *Genotyping*

Primer sequences for genotyping of *Ret*^{51} and *Ret*$^{51(C618F)}$ mice were as follows: forward P1 (5'-CGAGACCCGCCTGCTCCTCAACCGC-3') and reverse P2 (5'-CCTGCGGCGCCGGACGTCGCTTTCGCCAT-3') primers. 70-bp and 115-bp PCR products were amplified for the WT and knock-in alleles, respectively.

2.7 *Immunoprecipitation*

Transfected CHP126 cells were washed twice with ice-cold phosphate-buffered saline, pH7.4, and then extracted with immunoprecipitation buffer (10mM Tris-buffered saline, pH7.4, 1 mM EGTA, 1 mM EDTA, 150 mM NaCl, 1% TritonX-100, 0.5% NP-40, 5 mM sodium pyrophosphate, 10 mM NaF, 1mM Na3VO4, 10 mM *β-glycerophosphate, 1 mM phenylmethylsulfonyl fluoride, protease inhibitor and phosphatase inhibitor) for 10 min on ice. The detergent extracts were cleared of insoluble debris by centrifugation (20 min at 15000 g) at 4*°C. For immunoprecipitation, the supernatants were then incubated with 20 µl of protein G sepharose (50% gel slurry, GE Healthcare) and 1 µg of anti-RET antibody (C-20; Santa Cruz Biotechnology Inc., RRID: AB_631316) with gentle rocking for 2 hr at *4*°C. Immunocomplexes were then washed two times with immunoprecipitation buffer, eluted by boiling in sample buffer, resolved by SDS-PAGE, and analyzed by immunoblotting with the described antibodies.

2.8 *Isolation of cell surface proteins by biotin labeling*

Biotin labeling and isolation of cell surface wild-type or mutant RET proteins were performed following the *manufacturer's instructions (Pierce Cell Surface Protein Isolation Kit).* Cell surface proteins of transfected CHP126 cells were biotinylated with 0.25mg/ml Sulfo-NHS-SS-Biotion in PBS for 30 min at 4°C on a platform rotator. Isolation of biotinylated cell surface proteins was done by NeutrAvidin Agarose column.

2.9 *Immunoblotting*

Cell extracts or immunoprecipitates were subjected to SDS-PAGE in 6% mini.gels, and the separated proteins were transferred to nitrocellulose membranes (Advantec). The blots were then blocked with 2.5% skim milk or 2% bovine serum albumin in TBST (0.1% Tween20 in Tris-buffered saline) for 1 hr. The blots were next incubated with the primary antibody (mouse anti-Ret, 12EXY; Santa Cruz Biotechnology Inc., RRID:

AB_1128340) in the appropriate blocking buffer overnight at 4°C, washed 3×10 min with TBST, and then incubated with the appropriate horseradish peroxidase-conjugated secondary antibodies (1:40,000 dilution; goat-anti-mouse IgG, Jackson Immuno Research, RRID: AB_2307392) in blocking buffer for 1 hr at room temperature. The immunoblots were again washed 3×10 min with TBST and detected specific proteins with chemiluminescent substrate (SuperSignal West Dura, Thermo scientific).

2.10 *In situ hybridization*

In situ hybridization (ISH) was performed as described (Enomoto et al., 2004).

All riboprobes for ISH were synthesized using the DIG RNA Labeling Kit (Roche) as specified by the manufacturer. Digoxigenin-labeled cRNA probes were generated using a DNA fragment encompassing bases 402-848 of the *Calcitonin* cDNA (adenine of the initiator Met is assigned as 1) as template.

2.11 *Whole-mount immunostaining*

Dissected gut from embryos or P0 pups were fixed with 4% paraformaldehyde (PFA) in PBS containing 10mM phosphate buffer, pH7.4, 137 mM sodium chloride, and 2.7 mM potassium chloride overnight at 4°C and incubated in 1% Triton X-100 in PBS for 30 min at room temperature.

After fixation and permeabilization, the preparations were incubated in 0.1 M glycine in PBS for 2-6 hr and processed for immunohistochemistry.

For the preparations from P0 pups, blocking solution contains 5% skim milk, 5% DMSO, 1% Tween20 in PBS. The following antibodies were used: goat anti-hRET antibody (1:1000, C-20; Santa Cruz Biotechnology Inc., RRID: AB_631316); rat anti-mCherry [16D7] (1:500, EST202, KeraFAST); and guinea pig anti-Phox2b (1:1000, home-made, raised against the C-terminal region of WT Phox2b (Pattyn, Morin, Cremer, Goridis, & Brunet, 1997, RRID: AB_2313690). Secondary antibodies used were CF488 Donky anti-IgG (Biotium), CF568 goat anti-IgG (Biotium, RRID: AB_10559186) and Alexa Fluor 647 goat anti-guinea pig IgG (Thermo Fisher Scientific, RRID: AB_2735091).

2.12 *Enteric neuron counts*

Phox2b^{+} enteric neurons were counted in 10 areas at even intervals of the small intestine and the colon longitudinally (0.2 mm^2 each) and determined the density of enteric neurons

per organ from animals of each genotype.

2.13 *Statistical analysis*

Statistical analyses were performed in GraphPad Prism software (version 5, Software Inc.) and data are presented as means ± SEM. Comparison between individual groups were performed by Mann-Whitney U test.

ACKNOWLEDGMENTS

We thank Large (Laboratories: Animal Resource Development Unit & Genetic Engineering Team, RIKEN, CLST for their excellent technical assistance and the generation of germline transmitting chimeric mice from ES cells and T. Hirai for help with targeting vector construction and homologous recombination in ES cells. We also are grateful to D. Sipp for editing this manuscript.

REFERENCES

Accardo, G., Conzo, G., Esposito, D., Gambardella, C., Mazzella, M., Castaldo, F., . . . Pasquali, D. (2017). Genetics of medullary thyroid cancer: An overview. *Int J Surg, 41 Suppl 1*, S2-S6. doi:10.1016/j.ijsu.2017.02.064

Acton, D. S., Velthuyzen, D., Lips, C. J., & Hoppener, J. W. (2000). Multiple endocrine neoplasia type 2B mutation in human RET oncogene induces medullary thyroid carcinoma in transgenic mice. *Oncogene, 19*(27), 3121-3125. doi:10.1038/sj.onc.1203648

Asai, N., Iwashita, T., Matsuyama, M., & Takahashi, M. (1995). Mechanism of activation of the ret proto-oncogene by multiple endocrine neoplasia 2A mutations. *Mol Cell Biol, 15*(3), 1613-1619.

Carlomagno, F., Salvatore, G., Cirafici, A. M., De Vita, G., Melillo, R. M., de Franciscis, V., . . . Santoro, M. (1997). The different RET-activating capability of mutations of cysteine 620 or cysteine 634 correlates with the multiple endocrine neoplasia type 2 disease phenotype. *Cancer Res, 57*(3), 391-395.

Carlson, K. M., Dou, S., Chi, D., Scavarda, N., Toshima, K., Jackson, C. E., . . . Donis-Keller, H. (1994). Single missense mutation in the tyrosine kinase catalytic domain of the RET protooncogene is associated with multiple endocrine neoplasia type 2B. *Proc Natl Acad Sci U S A, 91*(4), 1579-1583.

Carniti, C., Belluco, S., Riccardi, E., Cranston, A. N., Mondellini, P., Ponder, B. A., . . . Bongarzone, I. (2006). The Ret(C620R) mutation affects renal and enteric development in a mouse model of Hirschsprung's disease. *Am J Pathol, 168*(4), 1262-1275.

Enomoto, H., Hughes, I., Golden, J., Baloh, R. H., Yonemura, S., Heuckeroth, R. O., . . . Milbrandt, J. (2004). GFRalpha1 Expression in Cells Lacking RET Is Dispensable for Organogenesis and Nerve Regeneration. *Neuron, 44*(4), 623-636.

Ito, S., Iwashita, T., Asai, N., Murakami, H., Iwata, Y., Sobue, G., & Takahashi, M. (1997). Biological properties of Ret with cysteine mutations correlate with multiple endocrine neoplasia type 2A, familial medullary thyroid carcinoma, and Hirschsprung's disease

phenotype. *Cancer Res, 57*(14), 2870-2872.

Lois, C., Hong, E. J., Pease, S., Brown, E. J., & Baltimore, D. (2002). Germline transmission and tissue-specific expression of transgenes delivered by lentiviral vectors. *Science, 295*(5556), 868-872.

Michiels, F. M., Chappuis, S., Caillou, B., Pasini, A., Talbot, M., Monier, R., . . . Billaud, M. (1997). Development of medullary thyroid carcinoma in transgenic mice expressing the RET protooncogene altered by a multiple endocrine neoplasia type 2A mutation. *Proc Natl Acad Sci U S A, 94*(7), 3330-3335.

Mulligan, L. M., Kwok, J. B., Healey, C. S., Elsdon, M. J., Eng, C., Gardner, E., . . . et al. (1993). Germ-line mutations of the RET proto-oncogene in multiple endocrine neoplasia type 2A. *Nature, 363*(6428), 458-460. doi:10.1038/363458a0

Pattyn, A., Morin, X., Cremer, H., Goridis, C., & Brunet, J. F. (1997). Expression and interactions of the two closely related homeobox genes Phox2a and Phox2b during neurogenesis. *Development, 124*(20), 4065-4075.

Reynolds, L., Jones, K., Winton, D. J., Cranston, A., Houghton, C., Howard, L., . . . Smith, D. P. (2001). C-cell and thyroid epithelial tumours and altered follicular development in transgenic mice expressing the long isoform of MEN 2A RET. *Oncogene, 20*(30), 3986-3994. doi:10.1038/sj.onc.1204434

Santoro, M., Carlomagno, F., Romano, A., Bottaro, D. P., Dathan, N. A., Grieco, M., . . . al, e. (1995). Activation of RET as a dominant transforming gene by germline mutations of MEN2A and MEN2B. *Science, 267*(5196), 381-383.

Schuchardt, A., D'Agati, V., Larsson-Blomberg, L., Costantini, F., & Pachnis, V. (1994). Defects in the kidney and enteric nervous system of mice lacking the tyrosine kinase receptor Ret. *Nature, 367*, 380-383.

Tsui-Pierchala, B. A., Ahrens, R. C., Crowder, R. J., Milbrandt, J., & Johnson, E. M., Jr. (2002). The long and short isoforms of Ret function as independent signaling complexes. *J Biol Chem, 277*(37), 34618-34625. doi:10.1074/jbc.M203580200

Wells, S. A., Jr., Chi, D. D., Toshima, K., Dehner, L. P., Coffin, C. M., Dowton, S. B., . . . et al. (1994). Predictive DNA testing and prophylactic thyroidectomy in patients at risk for multiple endocrine neoplasia type 2A. *Ann Surg, 220*(3), 237-247; discussion 247-250.

Wolfe, H. J., Melvin, K. E., Cervi-Skinner, S. J., Saadi, A. A., Juliar, J. F., Jackson, C. E., & Tashjian, A. H., Jr. (1973). C-cell hyperplasia preceding medullary thyroid carcinoma. *N Engl J Med, 289*(9), 437-441. doi:10.1056/NEJM197308302890901

Yin, L., Puliti, A., Bonora, E., Evangelisti, C., Conti, V., Tong, W. M., . . . Romeo, G. (2007). C620R mutation of the murine ret proto-oncogene: loss of function effect in homozygotes and possible gain of function effect in heterozygotes. *Int J Cancer, 121*(2), 292-300. doi:10.1002/ijc.22378

FIGURE LEGENDS

Figure 1. MTC-associated mutant RET51(C618F) exhibits ligand-dependent RET activation. (A) The domain structure of RET51 protein isoform. S, signal peptide; CLD, cadherin_like domain; CRD, cysteine_rich domain; TM, transmembrane domain; TKD, tyrosine kinase domain. (B) Phosphorylation of wild-type and mutant RET51. Neuroblastoma cell line CHP126 was infected by lentivirus carrying human wild-type RET51, RET51(C618F), RET51(C618R), or RET51(C620R). RET protein immunoprecipitated with anti-RET antibody was subjected to SDS-PAGE and probed with anti-phospho-RET (pTyr1062) antibody (higher panel). The amount of RET protein among the lanes was evaluated by probing with the anti-RET antibody (lower panel). (+) symbol indicates the presence of 50 ng/ml GDNF. (-) symbol indicates the absence of GDNF. (C) Cell surface expression level of RET51(C618F) protein. Cell surface proteins were labeled with biotin. Biotinylated protein immunoprecipitated with streptavidin conjugated to agarose was subjected to SDS-PAGE and probed with anti-RET antibody.

Figure 2. Generation of *Ret*^{51} or *Ret* $^{51\ (C618F)}$ knock_in allele. (A) Schematics of *Ret*^{51} or *Ret*$^{51(C618F)}$ knock_in strategy. Exon 1 is indicated by the black box. A gene cassette comprising floxed human *Ret51* or *Ret51(C618F)* cDNA with intron polyA, mCherry reporter, and neomycin resistance (Neo) expression cassette flanked by *FRT* sites, was introduced into exon1 of the mouse *Ret* locus. (B) Southern blot analysis. The DNA samples were digested with *NcoI* and hybridized with digoxigenin_labeled probe. The targeted clone (white arrow) displayed a recombined band with expected size. NC, negative control; PC, positive control. (C) Genomic DNA was extracted from mouse tails and analyzed PCR using primers P1 and P2 to detect Ret wild type allele (70 base pairs [bp] or knock_in allele 115 bp).

Figure 3. Characterization of RET conditional reporter mice.
(A) Wholemount staining of E14.5 colon of *Ret* $^{+/+}$ and *Ret* $^{51\ (C618F)/\ 51\ (C618F)}$ mouse fetuses detected by immunostaining with anti-human RET51 (green) and anti-Phox2b (magenta). (B) Scheme of Cre recombinase-mediated removal of floxed *Ret51* or *Ret51(C618F)*, simultaneously generating mCherry-knock-in allele. (C) Conditional deletion of *RET51* cDNA and the accompanied mCherry expression from the *Ret* locus.

In *Ret*$^{51/+}$ / *Actb::Cre* mice, mCherry fluorescent was directly visualized in E13.5 intestine and kidney. Each insert shows the zoom of the myenteric plexus and ureteric bud epithelia. Scale bars: 20 μm

Figure 4. *Ret*$^{51C618F)}$ homozygous mice do not show intestinal aganglionosis and renal agenesis. (A) Whole-mount Phox2b staining of enteric neurons at the rectum from P0 *Ret*^{51} and *Ret*$^{51\ (C618F)}$ homozygous mice. (B) Anatomical findings of urogenital organs of *Ret*^{51} and *Ret*$^{51\ (C618F)}$ homozygous mice at P0. Ad, adrenal grand; Bl, bladder; Ki, kidney. Scale bars: A, 50 μm; B, 1000 μm.

Figure 5. *Ret*$^{51C618F)/+}$ mice display increased numbers of enteric neurons and thyroid C cells. (A) Whole-mount Phox2b staining of enteric neurons in the proximal small intestine from P0 *Ret*$^{51/+}$ and *Ret*$^{51\ (C618F)/+}$ mice. (B) Quantification of Phox2b^{+} myenteric neurons in the proximal small intestine from P0 *Ret*$^{51/+}$ (n=4) and *Ret*$^{51\ (C618F)/+}$ mice (n=4). (C) In situ hybridization for calcitonin in the thyroid from aged (one-year-old) *Ret*$^{51/+}$ and *Ret*$^{51\ (C618F)/+}$ mice. Each right panel is the zoom of depicted region of left panel. (D) Quantification of calcitonin-expressing C cell area in the thyroid sections from aged *Ret*$^{51/+}$ (n=3) and *Ret*$^{51\ (C618F)/+}$ mice (n=3). (E) Quantification of C cell-hyperplastic follicle numbers in the thyroid from aged *Ret*$^{51/+}$ (n=4) and *Ret*$^{51\ (C618F)/+}$ mice (n=4). Scale bars: A, 50 μm; B, 100 μm.

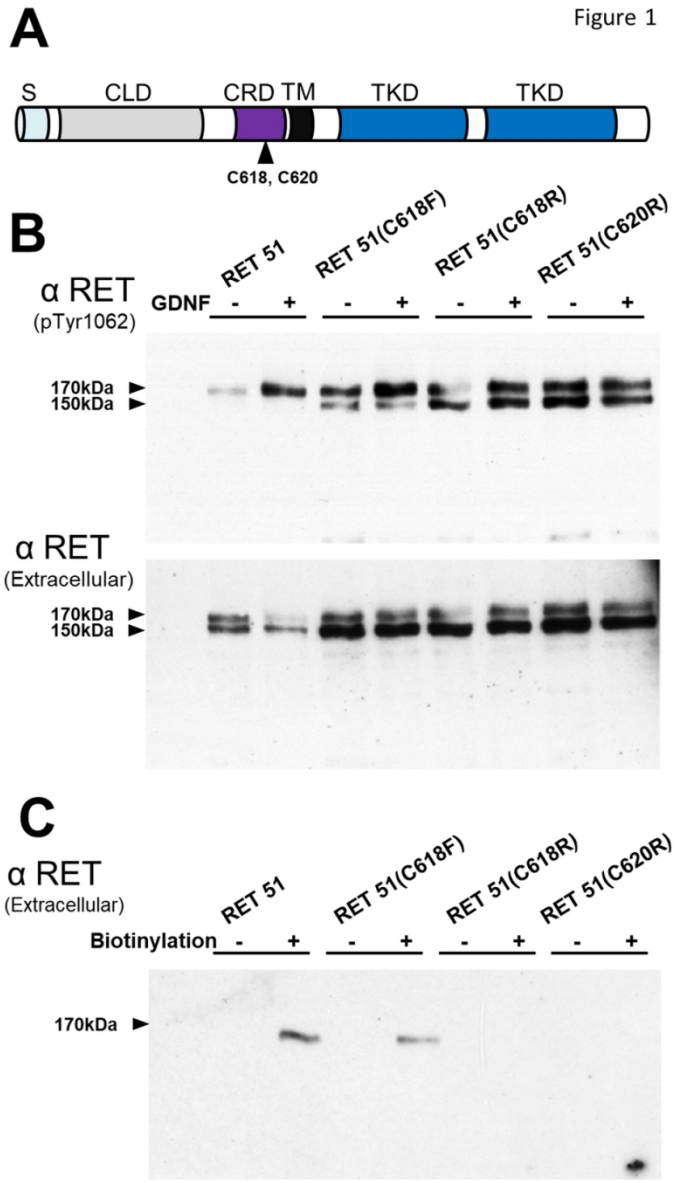

Figure 1

Figure 1. MTC-associated mutant RET51(C618F) exhibits ligand-dependent RET activation. (A) The domain structure of RET51 protein isoform. S, signal peptide; CLD, cadherin-like domain; CRD, cysteine-rich domain; TM, transmembrane domain; TKD, tyrosine kinase domain. (B) Phosphorylation of wild-type and mutant RET51. Neuroblastoma cell line CHP126 was infected by lentivirus carrying human wild-type RET51, RET51(C618F), RET51(C618R), or RET51(C620R). RET protein immunoprecipitated with anti-RET antibody was subjected to SDS-PAGE and probed with anti-phospho-RET (pTyr1062) antibody (higher panel). The amount of RET protein among the lanes was evaluated by probing with the anti-RET antibody (lower panel). (+) symbol indicates the presence of 50 ng/ml GDNF. (-) symbol indicates the absence of GDNF. (C) Cell surface expression level of RET51(C618F) protein. Cell surface proteins were labeled with biotin. Biotinylated protein immunoprecipitated with streptavidin conjugated to agarose was subjected to SDS-PAGE and probed with anti-RET antibody.

80x140mm (300 x 300 DPI)

Figure 2

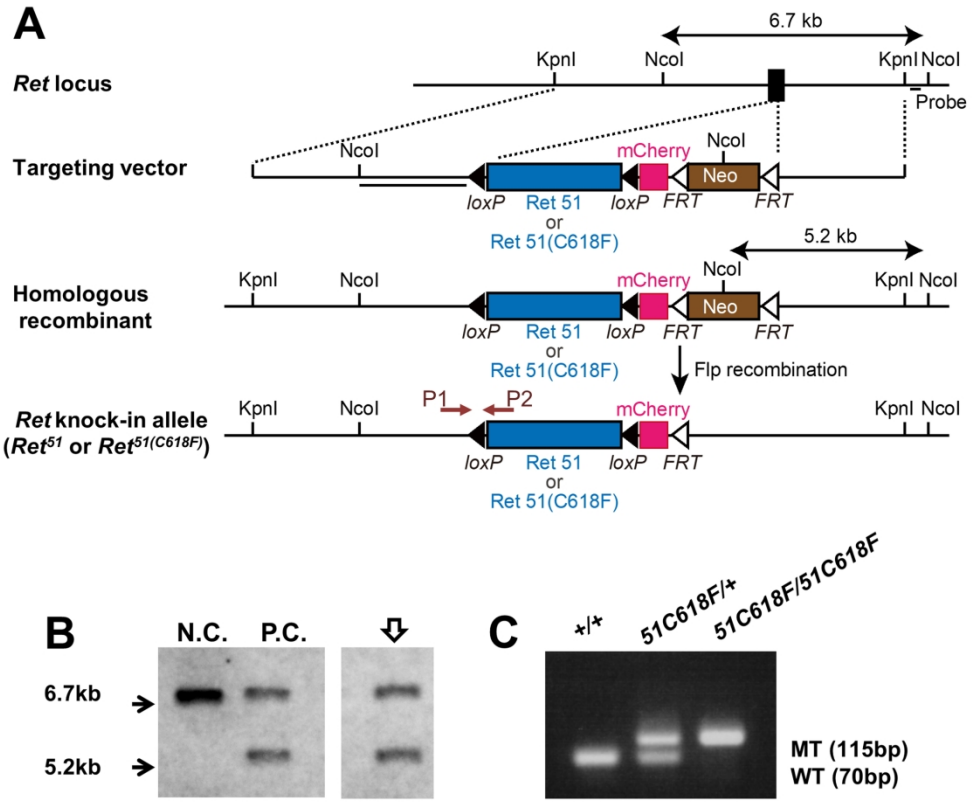

Figure 2. Generation of Ret51 or Ret 51 (C618F) knock-in allele. (A) Schematics of Ret51 or Ret51(C618F) knock-in strategy. Exon 1 is indicated by the black box. A gene cassette comprising floxed human Ret51 or Ret51(C618F) cDNA with intron polyA, mCherry reporter, and neomycin resistance (Neo) expression cassette flanked by FRT sites, was introduced into exon1 of the mouse Ret locus. (B) Southern blot analysis. The DNA samples were digested with NcoI and hybridized with digoxigenin-labeled probe. The targeted clone (white arrow) displayed a recombined band with expected size. NC, negative control; PC, positive control. (C) Genomic DNA was extracted from mouse tails and analyzed PCR using primers P1 and P2 to detect Ret wild type allele (70 base pairs [bp] or knock-in allele 115 bp).

190x175mm (300 x 300 DPI)

Figure 3

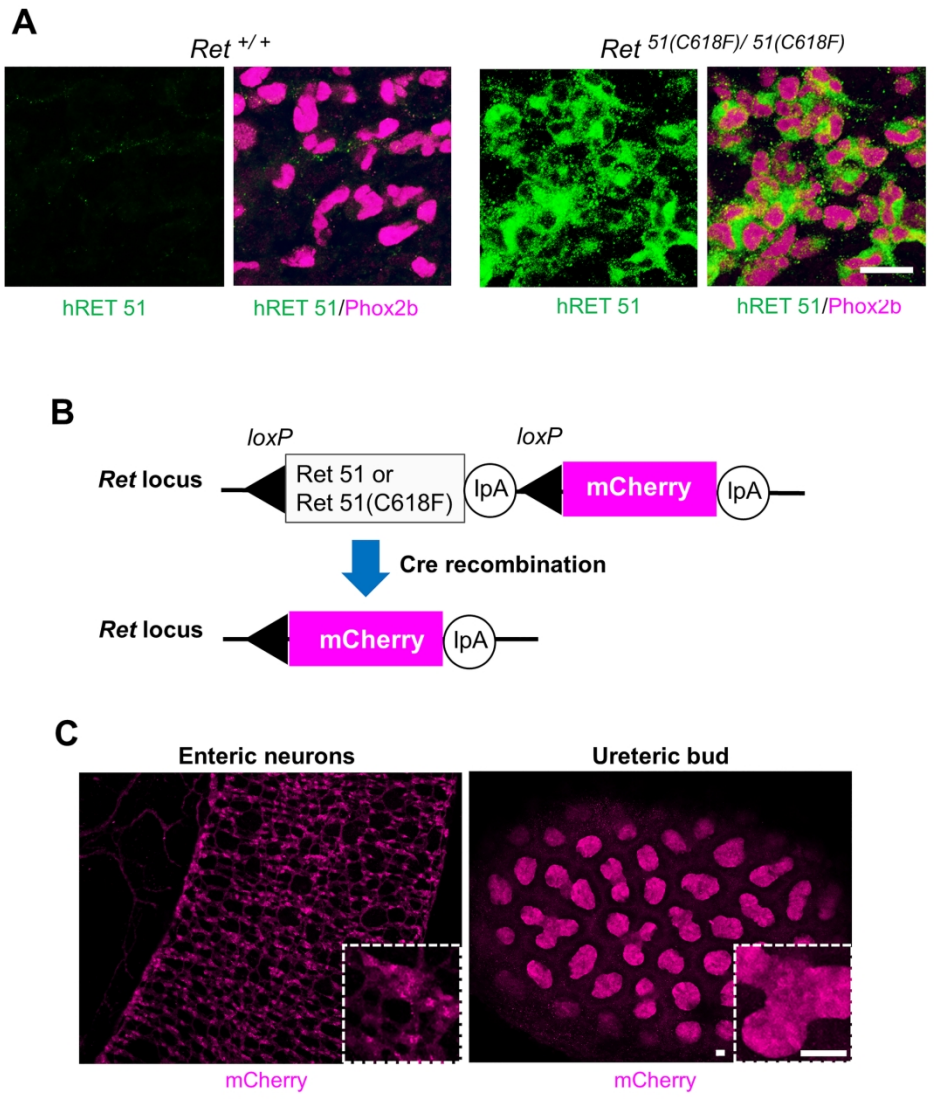

Figure 3. Characterization of RET conditional reporter mice.
(A) Wholemount staining of E14.5 colon of Ret +/ + and Ret 51 (C618F)/ 51 (C618F) mouse fetuses detected by immunostaining with anti-human RET51 (green) and anti-Phox2b (magenta). (B) Scheme of Cre recombinase-mediated removal of floxed Ret51 or Ret51(C618F), simultaneously generating mCherry-knock-in allele. (C) Conditional deletion of RET51 cDNA and the accompanied mCherry expression from the Ret locus. In Ret51/+ / Actb::Cre mice, mCherry fluorescent was directly visualized in E13.5 intestine and kidney. Each insert shows the zoom of the myenteric plexus and ureteric bud epithelia. Scale bars: 20 μm

180x216mm (300 x 300 DPI)

Figure 4

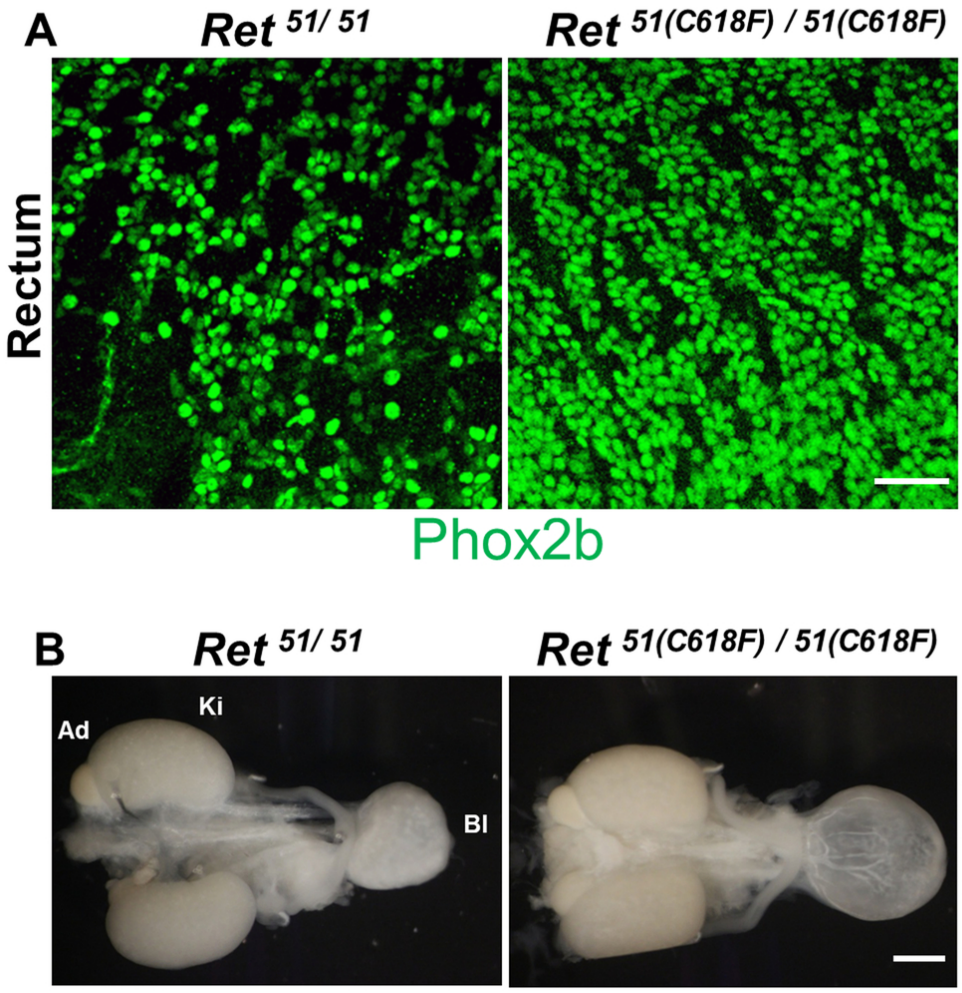

Figure 4. Ret51C618F) homozygous mice do not show intestinal aganglionosis and renal agenesis. (A) Whole-mount Phox2b staining of enteric neurons at the rectum from P0 Ret51 and Ret51 (C618F) homozygous mice. (B) Anatomical findings of urogenital organs of Ret51 and Ret51 (C618F) homozygous mice at P0. Ad, adrenal grand; Bl, bladder; Ki, kidney. Scale bars: A, 50 μm; B, 1000 μm.

85x98mm (300 x 300 DPI)

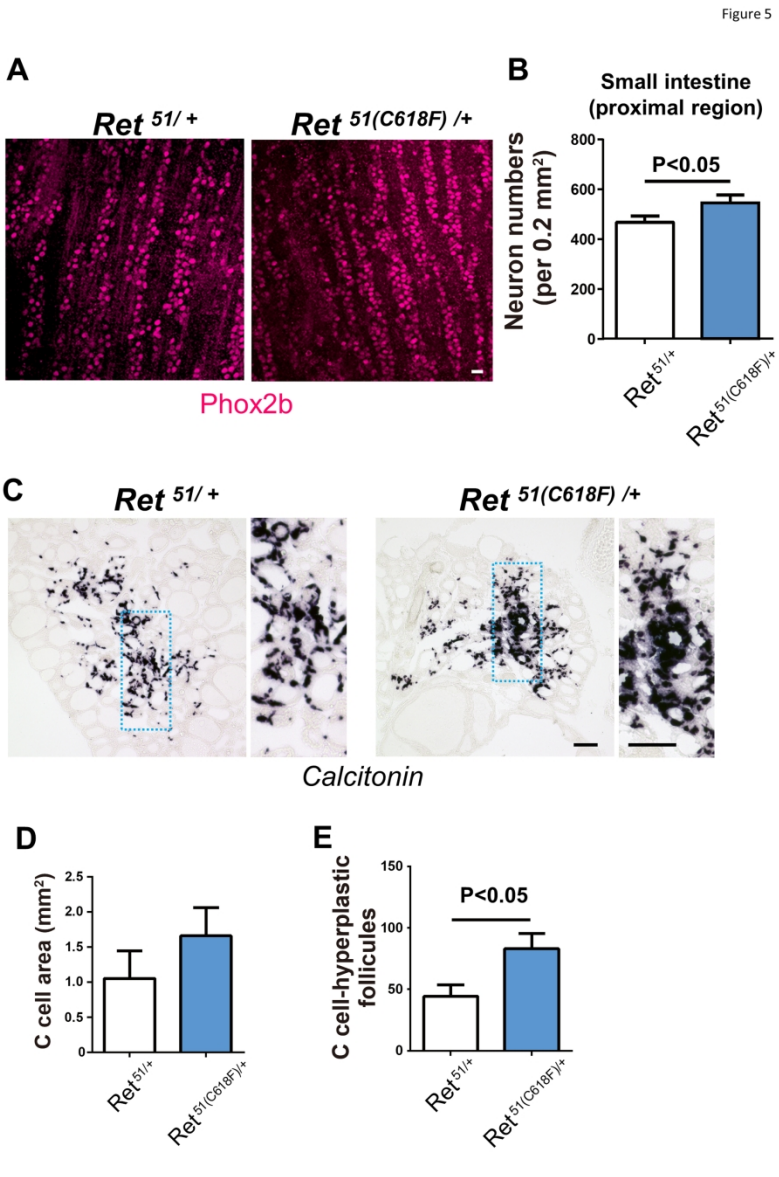

Figure 5. Ret51C618F)/+ mice display increased numbers of enteric neurons and thyroid C cells. (A) Whole-mount Phox2b staining of enteric neurons in the proximal small intestine from P0 Ret51/+ and Ret51 (C618F)/+ mice. (B) Quantification of Phox2b+ myenteric neurons in the proximal small intestine from P0 Ret51/+ (n=4) and Ret51 (C618F)/+ mice (n=4). (C) In situ hybridization for calcitonin in the thyroid from aged (one-year-old) Ret51/+ and Ret51 (C618F)/+ mice. Each right panel is the zoom of depicted region of left panel. (D) Quantification of calcitonin-expressing C cell area in the thyroid sections from aged Ret51/+ (n=3) and Ret51 (C618F)/+ mice (n=3). (E) Quantification of C cell-hyperplastic follicle numbers in the thyroid from aged Ret51/+ (n=4) and Ret51 (C618F)/+ mice (n=4). Scale bars: A, 50 μm; B, 100 μm.

190x275mm (300 x 300 DPI)